Characterising the Back-face Deformation of Ballistic Shields using an Augmented WorldSID Upper Limb

Julia E. de Lange, Liam J. Burrows, Jean-Sébastien Binette, Cheryl E. Quenneville

Abstract Shield back-face deformation (BFD) is the result of composite ballistic shields deflecting or absorbing a projectile and deforming towards the user. Back-face deformation can result in localised loading to the upper extremity, where the shield is supported. An anthropomorphic test device upper extremity was modified to quantify applied load due to shield BFD. Four vulnerable locations along the upper extremity were investigated – the hand, wrist, forearm, and elbow – for examining differing boundary conditions and their effect on resultant load. Fifteen shots were conducted on composite shields according to Level III ballistic test standards, with an average bullet velocity of 840.7 ± 5.0 m/s. The mean peak back-face velocity of the shield was 208.9 ± 44.6 m/s. Results showed minimal effect of anatomical location, with only the wrist forces exceeding the elbow (p = 0.004), suggesting a more simplified version of testing may be used for future safety tests. The average duration for all impacts was 0.569 ± 0.233 ms, with no significant differences among locations. This is the first step in developing injury criteria for the upper extremity resulting from behind shield blunt trauma and these data will be used for developing injury thresholds in post-mortem human surrogates.

Keywords anthropomorphic test device (ATD), back-face deformation (BFD), ballistic shields, behind armour blunt trauma (BABT), upper extremity

I. INTRODUCTION

Ballistic shields protect users from high velocity projectiles primarily by absorbing energy through material deformation. When a bullet strikes a composite shield, the shield plastically deforms along the woven pattern of the structure to absorb the bullet, a process termed back-face deformation (BFD). Portable shields are supported by the arm when used by defense personnel. Ballistic shields are typically evaluated per standards preventing projectile penetration [1]. There are currently no known standards that limit the allowable force transferred to the upper extremity through shield behind armour blunt trauma (BABT). Development of these standards are critical, as back-face deformation poses threats of injury in the context of helmets (skull fracture), so a similar response could be expected of the upper extremity [2]. This type of injury can lead to the user dropping the shield, putting them at greater exposure and potentially putting them at greater risk of injury. A standard does exist, however, for body armour, that defines a maximum static back-face signature (BFS) in clay backing material, taken as a pass/fail criterion [3]. The National Institue of Justice in the United States developed this widely-referenced standard, which specifies the allowable BFS for five levels of protection classifications (types II-IV), in which the backface deformation must not exceed 44 mm [3]. This standard was developed with respect to the torso as it was designed for body armour. As such, it cannot be directly applied to shield standards, which are in contact with a different anatomical area, likely with different injury thresholds.

Dynamic injury risk has been investigated for the upper extremity for automotive safety, falls prevention, and sports injury prevention; however, injury is highly dependant on joint orientation [4], loading rate and duration [5], and anthropometric size [6]. The upper extremity injury thresholds that have been developed are expected to vary substantially from that as a result of BFD, as these are focussed, high-force loading events, ocurring over a very short time period [7]. These injury thresholds are therefore unable to be directly applied to shield deformation.

Two known previous studies have investigated BFD of ballistic shields [7] [8]. Reference [7] aimed to develop an operational testing protocol to evaluate tactical ballistic shields to address the level of shield protection to

C. E. Quenneville is an Associate Professor (quennev@mcmaster.ca, (905) 525-9140 x 21797) in the School of Biomedical Engineering and the Department of Mechanical Engineering at McMaster University in Hamilton, Canada. J. E. de Lange is a PhD student and L. J. Burrows is a MASc student in the School of Biomedical Engineering at McMaster University in Hamilton, Canada. J.-S. Binette is a Scientist at Defence Research and Development Canada – Valcartier Research Centre in Quebec City, Canada.

prevent forearm and hand bone fractures [7]. They considered the distance between the back side of the shield and the upper extremity, termed stand-off distance, as a design parameter to optimise in future shield iterations. Results from this study produced peak resultant forces ranging from 4 to 16 kN as stand-off distance decreased from 40 to 30 mm, highlighting the need for further investigation as well as the development of injury tolerance criteria as a result of this loading mechanism. This study was a preliminary investigation of shield deformation but was limited to a single load cell with rigid boundary conditions.

Previous work from our lab has characterised the effects of two differing Level III ballistic shields on loading of an Anthropomorphic Test Device (ATD) hand and elbow [8]. The hand was modified to facilitate the addition of force sensors at this location and clamped onto a metal handle. The arm was supported on the proximal end at the mid-humerus, essentially a double-cantilevered system. This study investigated two different stand-off distances, resulting in peak forces up to 5.3 kN. However, small sized force sensors were employed that may not have captured the full deformation of the shield, and a direct comparison between boundary conditions was not possible due to differing shields with differing BFDs used in these impacts. As such, further investigation is required to independently study the effects of rapid shield deformation on upper extremity loading at vulnerable locations along the forearm.

Shield BFD can result in localised blunt loading to the upper extremity, where the shield is secured to the user. The objective of this work was to characterise behind shield loading to the upper extremity at four locations along the arm: the hand, wrist, forearm, and elbow. An augmented Worldwide Harmonized Side Impact Dummy (WorldSID, Humanetics Innovation Solutions, Farmington Hills, MI, USA) 50th percentile male upper extremity ATD was employed to investigate the effects of differing boundary conditions as a result of different anatomical impact locations.

II. METHODS

Anthropomorphic Test Device Used for Data Collection

The WorldSID 50th percentile male ATD upper limb was previously modified to add force sensors at four anatomical locations to quantify the localised, high-rate forces typical of behind shield blunt trauma [8]. This device is the most advanced side impact dummy to date and has been evaluated for its full body biofidelity under limited automotive conditions [9]. It has integrated instrumentation, including a 2-axis elbow load cell collecting moments in two directions (W50-71060S11, Humanetics Innovative Solutions, Farmington Hills, MI, USA) and a 6-axis forearm load cell, collecting forces and moments in all three directions (W50-71060DS11, Humanetics Innovative Solutions, Farmington Hills, MI, USA). In the present study the polyvinyl chloride (PVC) flesh of the surrogate was removed, and large force sensors (32.5 mm sensing diameter) were added to the hand, forearm, and elbow (model 200C20, PCB Piezotronics, MTS Systems Corporation, Depew, NY, USA). To avoid mechanical damage and potential overload, impacts directly to the integrated load cells were avoided. In these cases, inclusion of Humanetics-manufactured structural components replaced the integrated load cells of the WorldSID ATD, and the PicoCoulomB (PCB) sensors were mounted onto the ATD arm at the location of impact (Fig. 1). These force sensors had a low frequency response (-5%) and a high measurement range (up to 88.96 kN), making them a suitable measurement system for this application. For all other impacts, the integrated instrumentation was used (Table I). Due to the smaller anatomical location and physical mounting area requirements of these sensors, a smaller force sensor (16.5 mm sensing diameter) was used for the wrist impacts (model 201B05, PCB Piezotronics, MTS Systems Corporation, Depew, NY, USA). For all shots, the arm was placed 20 mm behind the back-face of the shield at the anatomical impact location of interest.

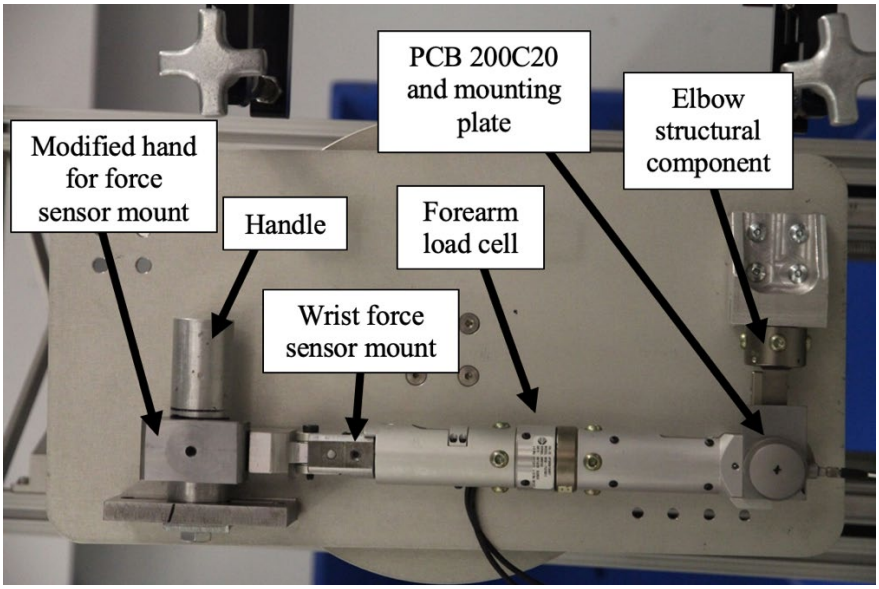

Fig. 1. Modified WorldSID ATD upper extremity to facilitate shield BABT data collection, positioned for elbow testing, with important modifications highlighted.

TABLE I
MEASURED PARAMETERS

Anatomical Location	Data Collected	Repetitions
Hand	PCB 200C20, Elbow 2-axis, Forearm 6-axis	4
Wrist	PCB 201B05, Elbow 2-axis, Forearm 6-axis	3
Forearm	PCB 200C20, Elbow 2-axis	4
Elbow	PCB 200C20, Forearm 6-axis	4

Due to a limited number of shots available, repetitions for each location varied to achieve at least three repetitions for each impact location. Each shot was presumed to be independent of one another. As such, only two elbow shots were conducted at the same impact location on different shields. All other shots were randomized in terms of shield placement and impact location.

Experimental Ballistic Testing

A 7.62mm North Atlantic Treaty Organization (NATO) ball projectile (9.6 g) was fired at nominal velocity of 838 ± 15 m/s, per the testing procedure of Ballistic Resistant Protective Materials associated with Level III threat type (NIJ-STD-0108.01) [10]. Two orthogonal high-speed cameras (Fastcam SA-X type 324K-M2), one positioned overhead and one camera parallel to the shot path captured the event at 30,000 fps to measure the back-face velocity and deformation of the shield. The bullet was fired from a universal receiver test barrel (Wiseman 09-2016(08), Bill Wiseman and Co. Inc., College Station, TX, USA), with a length of 559 mm and a right-hand twist rate of 1:305 mm. The bullet travelled 15 m down the test range, and velocity was measured using a Doppler radar (model BR-198 3502, Infinition Inc., Trois-Rivières, QC, Canada) and two photoelectric screens used as backup system (model 53131 A, Oehler Research Inc., Austin, TX, USA) that were spaced 1 m apart (Fig. 2). The yaw of the bullet just before the impact point was also assessed using high-speed video (36,000 fps, 1024x288 resolution) after each shot and if the angle of the bullet exceeded 5°, the shot was discarded. Shots were aligned using a laser sight through the universal receiver with the centre of the force sensor at the predetermined impact location (Fig. 3).

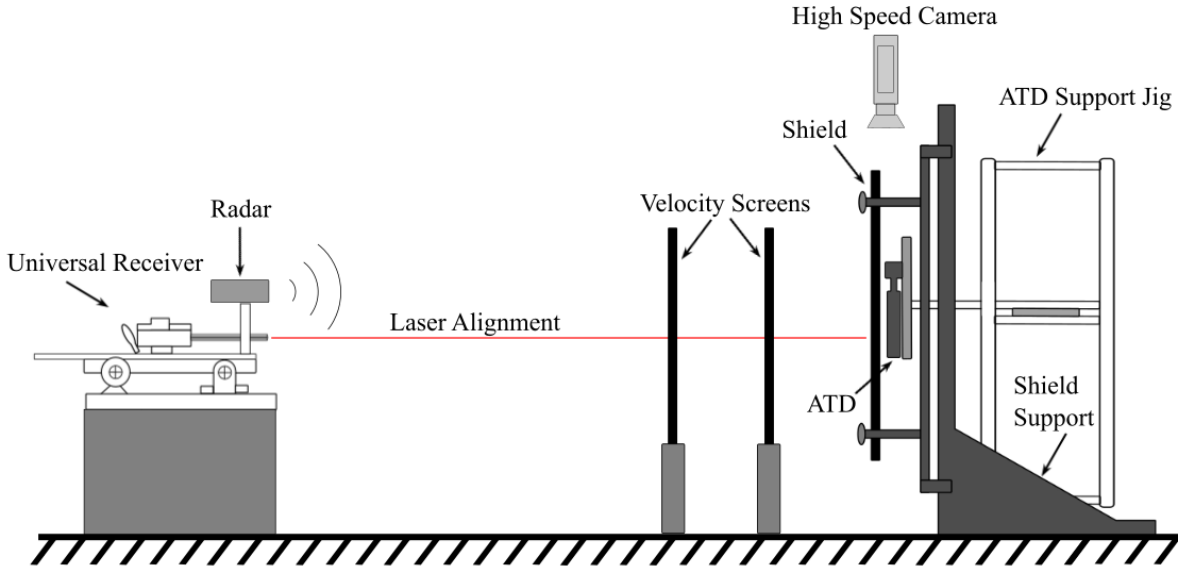

Fig 2. Schematic of the experimental setup, in which the bullet travelled down a 15 m path to the front face of the shield.

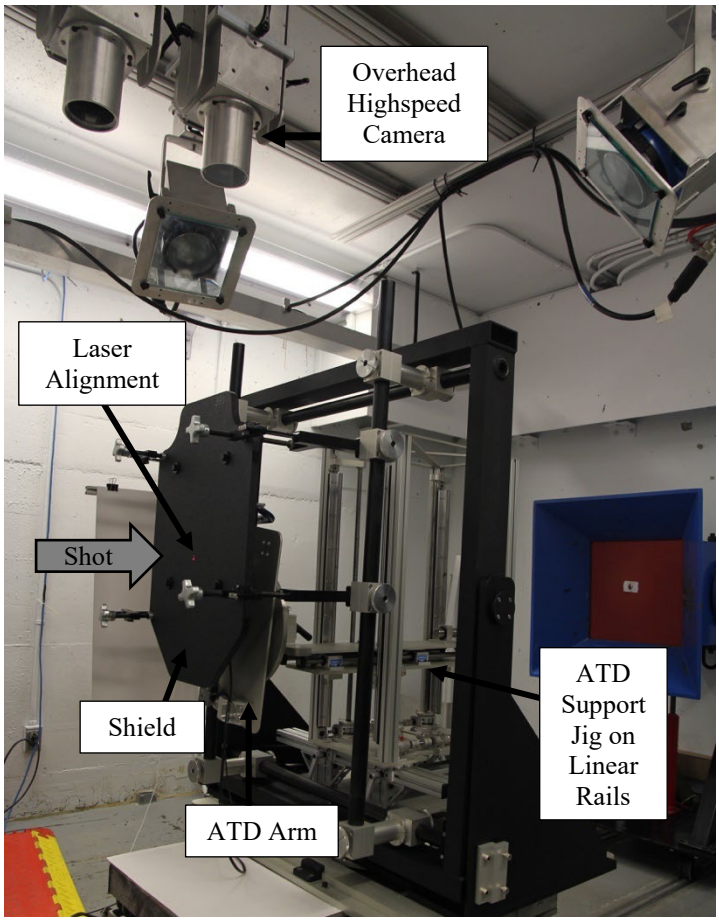

Fig. 3. Testing setup with the ATD upper extremity positioned behind the ballistic shield.

The trauma-attenuating foam backing, handles, and supporting hardware were all removed for ease of alignment in the testing jig and high-speed camera recording visibility. The shields were 508 mm wide and 762 mm tall and tapered at each of the four corners. Manufacturing information for the shields cannot be specified due to contract requirements.

Preliminary testing to determine the amount of shield back-face deformation showed that visible delamination from a singular shot typically extended approximately 60 mm. To minimise the effects of adjacent shots, each shot locations was placed a minimum of 150 mm apart from any previous shots, 120 mm away from

the shield edge, and 100 mm away from holes for supporting the shield via the arm. This allowed for each shot investigated to be independent from the previous shots, allowing for six shots per shield.

The arm was positioned in a customisable testing jig behind the shield, which had variability that allowed the target anatomical location to be laser aligned. The arm was mounted to a testing plate at the mid-humerus and rigidly attached to a handle, making a 90-degree bend at the elbow. This was confirmed through the use of a laser level. There was spacing between the back of the arm and front of the test plate to ensure contact between the arm and the test plate did not occur over the impact. This allowed for post-kinematic motion by allowing translation of the ATD after impact. This test setup also tested a rigid hand (crushing against a handle) and a cantilevered elbow, which represent two different yet realistic loading conditions.

The shield was mounted in front of the arm on an independent testing jig to ensure there was no global shield movement during each impact and was clamped at four locations along the perimeter of the shield. This allowed for the stand-off distance to be controlled for each test. The ATD support jig was on linear rails to allow for lateral movement post-impact (Fig. 3). All hardware was investigated prior to each test to ensure rigid attachment. Each impact location on the surrogate arm had at least three repetitions.

Data Analysis

The video footage was analysed in Photron FASTCAM Viewer Software (Photron USA Inc., San Diego, CA, USA) to calculate the BFD and velocity profiles (Fig. 4). For each shot, the impact was analysed (which occurred over 3-5 still frames) and extracted from the high-speed video, imported to Fiji ImageJ (Fiji, version 1.53f51, National Institutes of Health, Bethesda, MD, USA) and processed using the MTrackJ plugin. The peak deformation was identified within each frame and the frame rate (30,000 fps) determined the interval between still images, allowing for the calculation of back-face velocity between successive frames. The velocity was then averaged between the overhead and parallel videos for each shot to reduce error associated with obstruction of view caused by prior back-face deformation patterns. The same researcher repeated this process three times using the solid shape of the image rather than the blur of the polyurea coating, and the results were averaged. The jig travel distance after each impact was also recorded.

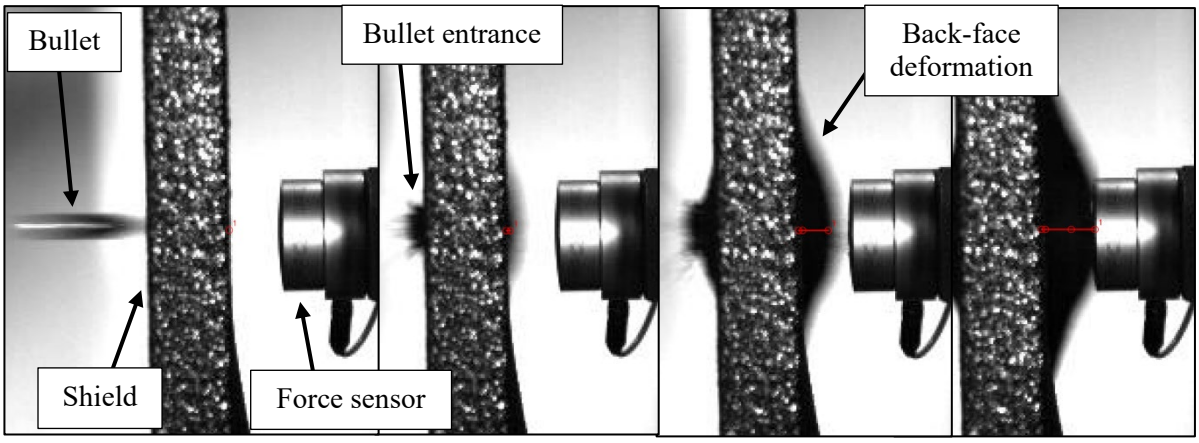

Fig. 4. High-speed video footage of the bullet impacting the shield, and the shield deformation as it impacted the force sensor.

An NI-PXIe-1082 Data Acquisition system (National Instruments, Austin, TX, USA) with a NI TB-4330 terminal block that sampled data from the strain-based integrated elbow and forearm load cells at 100 kHz, as well as a PXIe-4480 module to sample data from the PCB force sensors at 1 MHz were used for data collection. All force data were analysed in Matlab (MathWorks, Natick, MA, USA). The ATD data were dual-pass filtered using a second-order Butterworth low-pass filter with a cut-off frequency of 1,250 Hz, in accordance with industry testing standards [11-12]. A Fast Fourier Transform was performed to analyse the data in the frequency domain, which informed the filtering technique of the PCB data, in which a second-order Butterworth low-pass filter with a cut-off frequency of 40 kHz was used. Impact duration was calculated by finding the peak impact force and the impact was set to have started when the force reached 5% of this peak and concluded when the impact force decreased back down to 5% of the peak. All impact profiles were aligned by peak force. A one-way Analysis of Variance

(ANOVA) with post hoc Tukey test was conducted on peak force, duration of impact and impulse to compare among impact locations. A significance threshold was set at $\alpha = 0.05$.

III. RESULTS

The average bullet velocity at impact was 840.7 ± 5.0 m/s (mean ± SD) over the 15 total shots. High-speed video confirmed impacts were centred on the force sensor of interest. The mean peak back-face velocity of the shield was 208.9 ± 44.6 m/s, while the average deformation was 16.0 ± 3.6 mm. The peak forces for the hand, wrist, forearm, and elbow were 3750 ± 874 N, 5274 ± 1571 N, 3753 ± 819 N, and 2026 ± 492 N, respectively (Fig. 5a). Only the wrist location was significantly higher than the elbow ($p = 0.004$, Fig 5b). Among all impacts, the average duration was 0.569 ± 0.233 ms, with no significant differences among locations ($p > 0.48$, when comparing each anatomical location to one another, Fig.6). The average impulse for all anatomical locations was 0.553 ± 0.287 N*s (Fig. 7), also with no significant differences among anatomical locations ($p > 0.9$). The jig did not travel substantially after each impact (1.8 ± 1.2 cm).

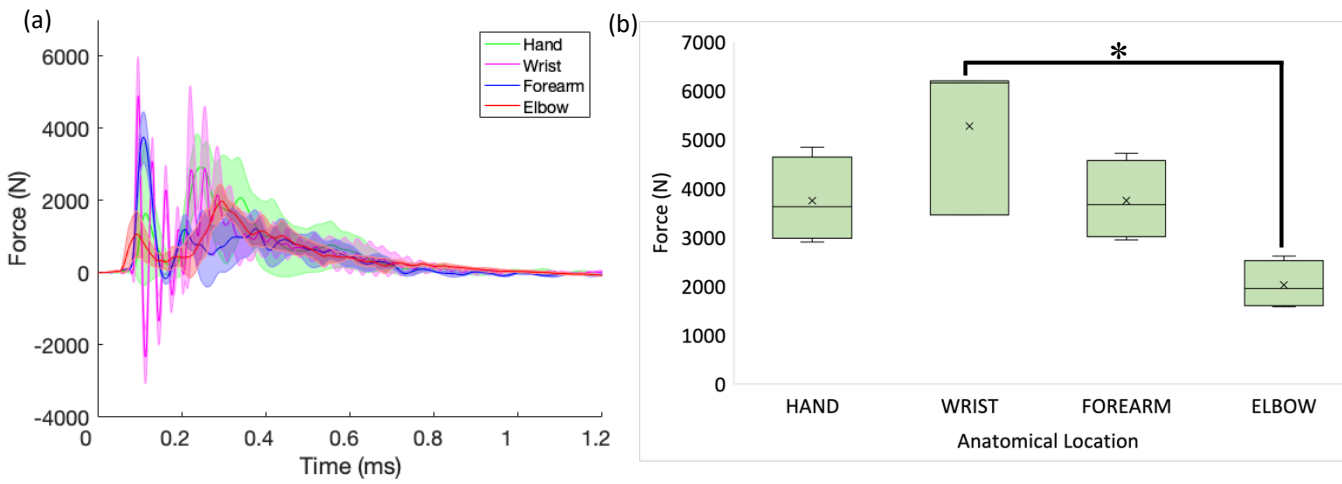

Fig. 5. Force collected at the location of impact (a) Filtered force-time traces, aligned by peak force for each anatomical impact location. The solid line represents the mean of each repeated impact, while the shaded region represents the standard deviation, and (b) Peak force at each anatomical location. (Note '*' denotes a significant finding).

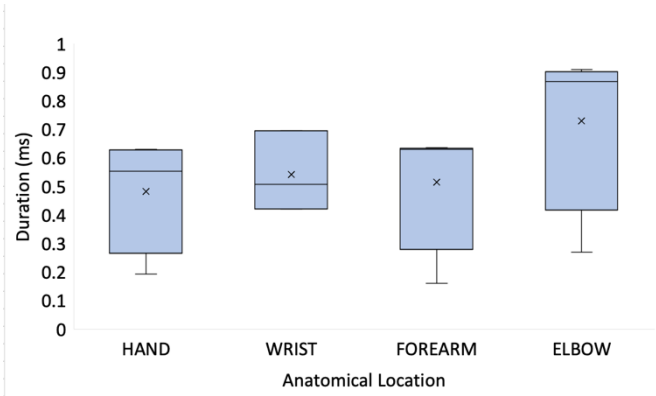

Fig. 6. Impact duration at each anatomical location.

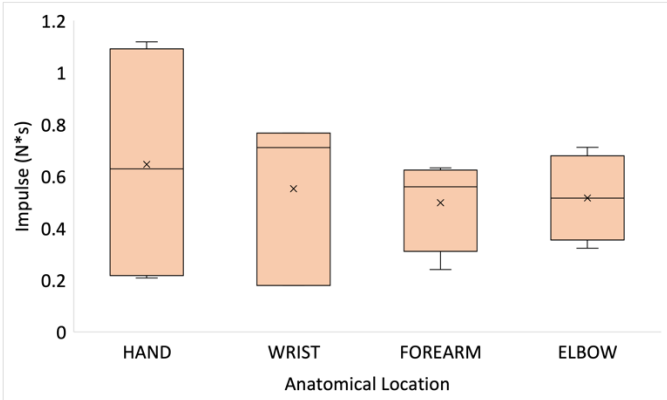

Fig. 7. Impulse at each anatomical location.

The integrated load cell moments were minimal (highest at forearm during the wrist impacts at 5.2 ± 0.8 Nm), highlighting the focal nature of these impact events.

IV. DISCUSSION

The generation of force-time curves for quantifying the BFD of shields is the first step in developing biomechanical assessments for this type of loading. The force generated during these impacts were as high as

approximately 6.2 kN over as short as 0.140 ms. Therefore, this impact event is substantially different from blunt ballistic impacts studied in the context of the thorax, in which forces generated were over 7 kN over several milliseconds [13] or the head, in which forces over 10 kN were recorded [2]. This represents the first known study to investigate the effect of anatomical impact location on BABT to the upper extremity, with the largest number of shots and the use of an instrumented surrogate to accurately capture this unique loading event.

The differing boundary conditions did not have a substantial effect on peak force recorded. However, the wrist impact location did record significantly higher forces (5274 ± 1571 N) than the elbow (2026 ± 492 N), meaning boundary conditions have some effect on the force transfer. This finding is surprising as the wrist was the only impact location that used a smaller sensing area and requires future investigation. Further, there was some resonance observed in the wrist load cell, consistent with a previous study [8]. This is likely from vibration of the sensor on the ATD arm resulting from a mounted resonance frequency, so these forces should be used with caution. The hand recorded the highest impact forces (3750 ± 874 N), unsurprising due to a much more rigid boundary condition than the double-cantilevered elbow, for example. The large standard deviations from the data are indicative of a high level of variability that was inherent with these tests, as the variation in shield material properties and the effects of repeated shots is unknown.

The average peak forces measured in the present study (1.6-6.2 kN) were in line with those reported in a previous study (2.3-5.3 kN) [8], with the current study providing a more robust investigation of the effects of anatomical location. However, the trends observed were similar. Reference [8] reported average peak elbow forces at the 20 mm stand-off distance as 3.6 kN (compared to 1.9 kN in the present study) and 5.3 kN at 30 mm stand-off distance of the hand (compared with 3.8 kN and 20 mm stand-off in the present study). However, the results presented herein are much less than those presented by [7] at the 20 mm stand-off distance (6-16 kN), meaning the boundary conditions have a significant effect on the resultant force. Behind shield blunt impacts resulted in significantly higher forces than loading produced in the automotive industry, such as those recorded in upper extremities under side airbag loading. The peak forearm force measures have been recorded for approximately 800 N [14].

The minimal moments that were measured in this study from the integrated forearm load cell (maximum average peak forearm moment of 5.2 ± 0.8 Nm from wrist impacts) was much smaller than those observed during automotive impacts to the forearm. The humerus resultant moment has been reported as high as 94 Nm in these impacts [14]. This demonstrates the highly focal nature of behind shield blunt trauma and requires further investigation into how this translates into injury potential. The primary limitation of this study was the presented boundary conditions of the ATD arm. Although ATDs are designed to be biofidelic in their respective direction of impact, they are stiffer than biological specimens [15], so the effects of anatomical location boundary conditions in post-mortem human surrogates (PMHS) is unknown but may be more significant. Further, additional instrumentation and facilitating mounting of that instrumentation may have produced overly rigid conditions that are not typical of the WorldSID ATD and biological upper extremities.

Next, the sampling rate of the high-speed video (30,000 fps) may not have been high enough to adequately capture the BFD profile of the shield as the time-to-peak of the force data was approximately 9 μs. As such, the shield velocity and deformation generated from the impacts should be treated as an estimate. The shield was secured in the testing apparatus using four clamps along the shield edges, with the arm placed 20 mm from the back-face of the shield. This is not how shields are typically supported in reality but was a necessary simplification to quantify these dynamic impacts and the resulting force transfer to a surrogate. The weight of the shield would be less than 3% of the force applied from back-face deflections. This test setup allowed for repeatable and reproducible conditions to comparatively assess the effects of impact location, while also allowing for the arm to experience some amount of post-impact translation. The deformation of the shield also occurred faster than the rearward movement of the shield, which was confirmed by high-speed imaging. Lastly, there were a limited number of available shots, and the effects of multiple shots on a single shield of this testing procedure are unknown. However, no trends of increasing force with shots conducted later in the testing sequence were observed to indicate any cumulative damage effects, and care was taken to avoid any shield delamination areas to be in contact in repeated shots.

To date, most research attention for upper limb ATDs has focused on the automotive industry, and current upper extremities have limited instrumentation, for example, the Hybrid III and Euro-SID 2 ATD's do not include instrumentation in the forearm. The WorldSID ATD is currently the most advanced upper extremity on the market

in terms of available embedded instrumentation. The biofidelity and validation of the WorldSID for this application remains unknown; however, match-pair testing with this surrogate and PMHS in the future will allow for assessment of the biofidelity of this augmented ATD and discern whether it is an appropriate tool for assessing injury risk.

The loading rate, magnitude, orientation of loading, and duration vary substantially from automotive impacts, meaning the injury mechanism and threshold likely differ as well. There are no known upper extremity injury threshold studies in the relevant loading direction that address the high-rate, short-duration loads that resulted from this study. As compared to side-impacts resulting from airbags for automotive applications, it is likely the injury limits would be higher due to the shorter duration of loading [5]. There is a gap in the literature where no dynamic injury criteria for ballistic impact events exists for the upper extremity, which will need to be developed for shield standards and designs in the future. Behind armour blunt trauma forces may be anywhere between two and 10 times greater than those of automotive conditions. The peak force observed in this study are in the range of those expected to cause upper limb fractures, highlighting the need for these investigations [3][16]. The present work presents the first known study of its kind to characterise impacts as a result of BABT at four anatomical locations along the upper extremity, which will provide the basis for development of injury criteria on PMHSs. The results from this study will be used to replicate impacts in a laboratory-based setting in order to develop injury thresholds.

V. CONCLUSIONS

The BFD characteristics of ballistic shields were investigated for potential risk of behind shield blunt trauma to the upper extremity. The BFD characteristics of the shield (peak force and duration of impact) and the anatomical region to protect differed from documented behind armour blunt trauma scenarios involving helmets and body armour, so standards specific to shields' interaction with the arm are needed. As there were minimal variations among anatomical impact location on the arm, this may offer the opportunity for a more simplified surrogate to be used for evaluating shield capabilities when developing a test standard. However, the double-cantilevered elbow may need to be assessed with greater biofidelic representation.

This work represents the first robust analysis of shield deformation as it pertains to BABT. The data collected will provide a basis for generating injury limits and represents the first step in developing standards defining the allowable force/impulse due to BFD of shields to optimise protective capabilities while minimising weight.

VI. ACKNOWLEDGEMENT

The authors would like to thank Benoit Gauthier and Steven Kelly (Defense Research and Development Canada) for their contributions to this work, and Defense Research and Development Canada for funding this study.

VII. REFERENCES

[1] Cannon, L. (2001). Behind Armour Blunt Trauma – An Emerging Problem. J. R. Army Med. Corps, 147(1): pp.87-96.
[2] Mukasey, M., Sedgwick, J., Hagy, D. (2008) National Institute of Justice, *Ballistic Resistance of Body Armor, NIJ Standard 0101.06,* Washington, DC.
[3] Duma, S., Schreiber, P., McMaster, J., Crandall, J., Bass, C. (2002). Fracture tolerance of the male forearm: the effect of pronation versus supination. *Proceedings of the Institution of Mechanical Engineers, Part D: Journal of Automobile Engineering.* 8(216): pp.649-654.
[4] Martinez, A., Chakravarty, A., Quenneville, C.E. (2018). The effect of impact duration on the axial fracture tolerance of the isolated tibia during automotive and military impacts. *Journal of the Mechanical Behavior of Biomedical Materials,* 78: pp.315-320.
[5] Amis, A., Miller, J. (2018). The mechanisms of elbow fractures: an investigation using impact tests in vitro. *Injury*, 26(3): pp.315-320.
[6] Bolduc, M., Anctil, B. (2010). Improved test methods for better protection: A BABT protocol proposal for STANAG 2920. *Proceedings in Personal Armour Systems Symposium (PASS),* Quebec, Canada.
[7] Steinmann, N., de Lange, J.E., Binette, J.-S., Quenneville, C.E. (2021). Quantification of Behind Shield Blunt Trauma Impacts Using a Modified Upper Extremity Anthropomorphic Test Device. *J. Biomech. Eng*, 144(9):091010
[8] Rhule, H., Moorhouse, K., Donnelly, B., Stricklin, J. (2009). *Comparison of WorldSID and ES-2re biofidelity using an updated biofidelity ranking system.* National Highway Traffic Safety Administration.
[9] Stewart, J. (1985) National Institute of Justice, *Ballistic Resistance Protective Materials, NIJ Standard 0108.01.*

[10] NATO (2006) Procedures for Evaluating the Protection Level of Logistic and Light Armored Vehicles, *Allied Engineering Publication,* 2(55)
[11] Kemper, A. (2013) Response corridors for the medial-lateral compressive stiffness of the human arm: Implications for side impact protection. Accident Analysis and Prevention, 50: pp.204-222.
[12] Bir, C., Lance, R., Stojsih-Sherman, S., Cavanaugh, J. (2017). Behind armour blunt trauma: recreation of field cases for the assessment of backface signature testing. *In 30th International Symposium on Ballistics,* Long Beach, California, USA.
[13] Weisenbach, C., Logsdon, K., Salzar, R., Chancey, V., Brozoski, F. (2018). Preliminary investigation of skull fracture patterns using an impact representative of helmet back-face deformation. Military Medicine, Suppl_1(183): pp.293-297.
[14] Duma, S., Boggess, B., Crandall, J., MacMahon, C. (2003). Injury risk function for the small female wrist in axial loading. Accident Analysis & Prevention, 6(35): pp.869-875.
[15] Quenneville, C.E., Dunning, C. (2012). Evaluation of the biofidelity of the HIII and MIL-Lx lower leg surrogates under axial impact loading. Traffic Injury Prevention, 13(1): pp.81-85.
[16] Duma, S., Schreiber, P., McMaster, J., Crandall, J., Bass, C., Pilkey, W. (1999). Dynamic injury tolerance for long bones of the female upper extremity. The Journal of Anatomy, 3(194): pp.463-471.